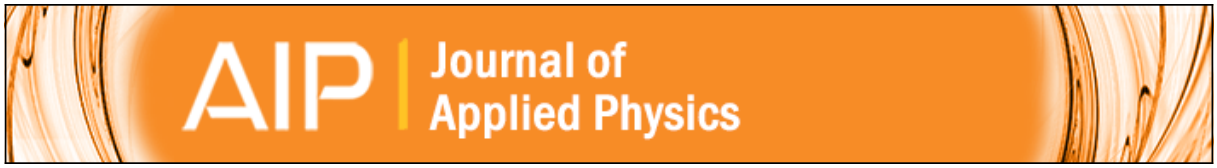


# Optical characterization of ZnSe epilayers and Zn Cd Se Zn Se quantum wells grown on Ge Ge 0.95 Si 0.05 Ge 0.9 Si 0.1 Si virtual substrates

J. T. Ku, M. C. Kuo, J. L. Shen, K. C. Chiu, T. H. Yang, G. L. Luo, C. Y. Chang, Y. C. Lin, C. P. Fu, D. S. Chuu, C. H. Chia, and W. C. Chou

Citation: Journal of Applied Physics **99**, 063506 (2006); doi: 10.1063/1.2181267
View online: http://dx.doi.org/10.1063/1.2181267
View Table of Contents: http://scitation.aip.org/content/aip/journal/jap/99/6?ver=pdfcov
Published by the AIP Publishing

**Articles you may be interested in**

Band alignment and excitonic localization of ZnO / Cd 0.08 Zn 0.92 O quantum wells
J. Appl. Phys. **107**, 093523 (2010); 10.1063/1.3359720

Quantum-confined Stark effects in the m -plane In 0.15 Ga 0.85 N Ga N multiple quantum well blue light-emitting diode fabricated on low defect density freestanding GaN substrate
Appl. Phys. Lett. **91**, 181903 (2007); 10.1063/1.2802042

Stark effect and oscillator strength in a Si 1 x Ge x Si quantum disk
J. Appl. Phys. **101**, 093709 (2007); 10.1063/1.2719005

Photoluminescence and built-in electric field in Zn O Mg 0.1 Zn 0.9 O quantum wells
Appl. Phys. Lett. **90**, 132113 (2007); 10.1063/1.2716367

Photocurrent and transmission spectroscopy of direct-gap interband transitions in Ge Si Ge quantum wells
Appl. Phys. Lett. **89**, 262119 (2006); 10.1063/1.2425032


Re-register for Table of Content Alerts

Create a profile.

Sign up today!

[This article is copyrighted as indicated in the article. Reuse of AIP content is subject to the terms at: http://scitation.aip.org/termsconditions. Downloaded to ] IP: 140.113.38.11 On: Thu, 01 May 2014 02:05:31

# Optical characterization of ZnSe epilayers and ZnCdSe/ZnSe quantum wells grown on $Ge/Ge_{0.95}Si_{0.05}/Ge_{0.9}Si_{0.1}/Si$ virtual substrates

J. T. Ku, M. C. Kuo, J. L. Shen, and K. C. Chiu
*Department of Physics, Chung Yuan Christian University, Chung-Li, Taiwan 32023, Republic of China*

T. H. Yang, G. L. Luo, and C. Y. Chang
*Department of Electronics Engineering, National Chiao Tung University, Hsin-Chu, Taiwan 30010, Republic of China*

Y. C. Lin, C. P. Fu, D. S. Chuu, C. H. Chia, and W. C. Chou[a)]
*Department of Electrophysics, National Chiao Tung University, Hsin-Chu, Taiwan 30010, Republic of China*

(Received 26 July 2005; accepted 31 January 2006; published online 22 March 2006)

Several approaches have been employed to grow high-quality ZnSe epilayers on $Ge/Ge_{0.95}Si_{0.05}/Ge_{0.9}Si_{0.1}/Si$ virtual substrates. The ZnSe epilayers were characterized by photoluminescence spectroscopy. Migration enhanced epitaxy and inserting an *in situ* thermal annealing ZnSe buffer layer effectively reduced the intensity of deep level emissions from the ZnSe epilayer grown on a 6°-tilted $Ge/Ge_{0.95}Si_{0.05}/Ge_{0.9}Si_{0.1}/Si$ virtual substrate. Optimized conditions for growing high-quality ZnSe were used to deposit ZnCdSe/ZnSe multiple quantum wells on $Ge/Ge_{0.95}Si_{0.05}/Ge_{0.9}Si_{0.1}/Si$ virtual substrates. Photoluminescence spectroscopy revealed quantum-confinement effect in the ZnCdSe multiple quantum wells. The evolution of the exciton emission peak energy and the linewidth as a function of temperature indicate a low density of localized sites in the sample with a well width of 1 nm. In the high-temperature regime, the thermal quenching of the excitonic emission intensity from ZnCdSe quantum well structures was governed by the thermal activation of carriers from quantum-well-confined states into barrier states. © *2006 American Institute of Physics*. [DOI: 10.1063/1.2181267]

## I. INTRODUCTION

ZnSe-based heterostructures have been intensively studied because they have practical applications in blue-green optoelectronic devices.[1,2] GaAs is the most used substrate in the fabrication of ZnSe-based optical devices because the lattice mismatch between GaAs and ZnSe is only 0.27%. However, efforts have been also made to grow ZnSe on a Si substrate,[3–6] which is less expensive and yields mechanical strength and thermal conductivity. Moreover, the successful growth of ZnSe-based multilayer structures on Si substrates enables the monolithic integration of II-VI optical devices and conventional Si integrated-circuit technology. Nevertheless, the large lattice mismatch (4.3%) and the difference between the thermal expansion coefficients of ZnSe and Si make the growth of high-quality ZnSe-based materials difficult.

The authors have already established that the use of a $Ge/Ge_{0.95}Si_{0.05}/Ge_{0.9}Si_{0.1}$ buffer layer[7] considerably improves the crystalline quality of a ZnSe epilayer on Si substrates.[8] From the low-temperature photoluminescence (LT-PL) spectroscopy revealed that the intensity of deep level emission (DLE) in a ZnSe thin film grown on a substrate with a 2° off-cut angle tilted from (100) toward the in-plane [110] direction is much lower than that associated with a 0°-tilted substrate. Furthermore, atomic interdiffusion of Ge buffer into the ZnSe epilayers has also been suppressed by using the 2°-tilted substrate. Although the DLE intensity from the ZnSe thin film grown on a 2°-tilted substrate is lower than that of a sample grown on a 0°-tilted substrate, room for improvement remains. Therefore, in current study, several methods such as varying the off-cut angle of the substrate, using a low-temperature migration enhance epitaxy (LT-MEE),[9] and the insertion of a buffer[10] were attempted to obtain high-quality ZnSe epilayers on $Ge/Ge_{0.95}Si_{0.05}/Ge_{0.9}Si_{0.1}/Si$ substrate (Ge/Si virtual substrate).

As demonstrated by the practical light-emitter devices, many semiconductor devices must take the advantages of multiple quantum well (MQW) structures for optimal device performance. Although several studies of the growth of a ZnSe thin film on a Si substrate have been conducted, ZnSe-related quantum structures on a Si substrate have not yet been reported. This lack motivates the investigation of the optical characteristics of ZnCdSe QWs grown on the Ge/Si virtual substrate. The ternary compound ZnCdSe is commonly used as a well material in ZnSe-based QW structures. Band gap can be easily engineered by choosing the Cd contents. Several studies have been performed on this alloy[11,12] and its QW system.[13–15] In particular, understanding the emission mechanism in these materials is important, from the perspectives of both fundamental physics and the design of practical devices. Accordingly, PL measurement was measured as a function of temperature to investigate the emission efficiencies.

[a)]Author to whom correspondence should be addressed; electronic mail: wuchingchou@mail.nctu.edu.tw

 © 2006 American Institute of Physics

[This article is copyrighted as indicated in the article. Reuse of AIP content is subject to the terms at: http://scitation.aip.org/termsconditions. Downloaded to ] IP: 140.113.38.11 On: Thu, 01 May 2014 02:05:31

TABLE I. Sample parameters and intensity ratios of the donor-bound exciton emission to deep level emission for the ZnSe epilayers. FWHM is the full width at half maximum of PL due to the donor-bound exciton.

| Sample | Substrate tilted angle (°) | Structure | Thickness of HT-ZnSe | Ratio of $D^0X$ to DLE | FWHM (meV) |
|---|---|---|---|---|---|
| A | 0 | HT-ZnSe | 1 $\mu$m | 26 | 8.2 |
| B | 4 | HT-ZnSe | 1 $\mu$m | 43 | 8.5 |
| C | 6 | HT-ZnSe | 1 $\mu$m | 98 | 5.2 |
| D | 6 | HT-ZnSe +LT-MEE | 1 $\mu$m | 238 | 4.9 |
| E | 6 | HT-ZnSe +LT-ZnSe buffer +LT-MEE | 900 nm | 417 | 4.9 |

In this work, the optical properties of a series of ZnSe epilayers grown on tilted Ge/Si virtual substrates were systematically examined. LT-PL measurements were made to evaluate the quality of ZnSe epilayers. The LT-MEE and insert of an *in situ* annealed ZnSe buffer layer result in high crystallinity. The method was then adopted to grow ZnCdSe/ZnSe MQWs on the Ge/Si virtual substrate. The optical properties of the MQW samples were studied. The effect of temperature on the emission efficiencies was analyzed using the Arrhenius plot.

## II. EXPERIMENT

The Ge/Si virtual substrates were grown by ultrahigh vacuum chemical vapor deposition. The details of growth were described in our previous papers.[7,8] The Ge/Si virtual substrate comprises of a Si substrate wafer, a $Ge_{0.9}Si_{0.1}$ layer (0.8 $\mu$m), a $Ge_{0.95}Si_{0.05}$ layer (0.8 $\mu$m), and a Ge layer (1 $\mu$m). The upward-propagating threading dislocation was terminated effectively at the interface between $Ge_{0.95}Si_{0.05}/Ge_{0.9}Si_{0.1}$ and $Ge/Ge_{0.95}Si_{0.05}$. The Ge layer with a low density of dislocations and a smooth surface.[7] was then a good template for the growth of ZnSe-related structures. In this study, *p*-Si substrate wafers with 0°, 4°, and 6° off-cut angles tilted from (100) toward the in-plane [110] direction were used. The Ge/Si virtual substrates were cleaned by dipping in acetone for 1 min and then in isopropyl alcohol for 1 min, followed by rinsing in de-ionized water for 5 min. The final dip in solutions of 10% HF left the substrate surface hydrophobic prior to loading. The substrate was then mounted with indium on a molybdenum block and transferred into the ultrahigh vacuum molecular beam epitaxy (MBE) system.

The Veeco-Applied-EPI 620 MBE system was utilized to grow the ZnSe-based structures on the Ge/Si virtual substrates. Solid sources of Zn (6*N* purity), Se (6*N* purity), and Cd (6*N* purity) were used for growth. The cell temperatures of Zn, Se, and Cd were 300, 175, and 220 °C, respectively. The substrate surface temperature was controlled at 250 °C [low temperature (LT)] and 300 °C [high temperature (HT)] throughout the growth process. The pressure of the growth chamber was lower than $5\times10^{-9}$ torr during the growth. Prior to ZnSe growth, the substrate was heated to 450 °C for 30 min to remove the residual oxide in the substrate. In this case, a $(2\times1)$ reconstructed (100) Ge surface was observed by the reflection high-energy electron diffraction. The substrate temperature was then reduced to 250 °C. During this period, the Zn shutter was opened to provide the Zn atoms. The purposes are to saturate the dangling bonds on the Ge surface and to prevent the formation of amorphous $GeSe_2$ (Ref. 3) during the ZnSe growth.

The parameters of five ZnSe epilayer samples are listed in Table I. Sample A is a 1 $\mu$m thick HT-ZnSe epilayer grown directly on a 0°-tilted Ge/Si virtual substrate, whereas samples B and C are grown on a 4°- and a 6°-tilted Ge/Si virtual substrate, respectively. Sample D is a 1 $\mu$m thick HT-ZnSe epilayer on a 6°-tilted Ge/Si virtual substrate with a LT-MEE layer. Sample E is a 900 nm thick HT-ZnSe grown on a LT-MEE layer+6°-tilted Ge/Si virtual substrate, with an inserted 100 nm thick LT ZnSe buffer layer annealed *in situ* at 400 °C for 10 min at a growth chamber pressure of $5\times10^{-9}$ torr. The method for growing the LT-MEE layer was as follows. First, open the Zn shutter to expose Zn atoms for 5 s; second, close the Zn shutter for 5 s; third, expose the Se atomic source for 5 s; and, finally, close the Se shutter for 5 s. This MEE process was repeated for about 3 min. The estimated thickness of the LT-MEE layer of ZnSe was 6 monolayers.

Good-quality ZnCdSe quantum structures should be growable under the optimized growth condition of the ZnSe epilayer. Therefore, the structure for the growth of sample E, which will later be established to be the best-quality ZnSe epilayer, was used to grow the $Zn_{1-x}Cd_xSe/ZnSe$ MQWs. The ZnCdSe/ZnSe MQWs were grown on an initial structure that is similar to that of sample E (LT-ZnSe buffer +LT-MEE layer+6°-tilted Ge/Si virtual substrate), but 500 nm of HT-ZnSe was deposited prior to the growth of five-period QW structures, as shown in Fig. 1. A ZnCdSe epilayer was also grown under the same conditions for reference. The proportion of Cd incorporated in ZnCdSe and its QW structures is about 17%, as determined by energy dispersive x-ray measurement. Three MQW samples with well widths ($L_w$'s) of 1, 3, and 5 nm were grown. The barrier thickness was fixed at 20 nm.

The 325 nm line of a He–Cd laser was used as an excitation source for PL spectroscopy, and the emission from the sample was analyzed using the SPEX 1403 double grating

[This article is copyrighted as indicated in the article. Reuse of AIP content is subject to the terms at: http://scitation.aip.org/termsconditions. Downloaded to ] IP: 140.113.38.11 On: Thu, 01 May 2014 02:05:31

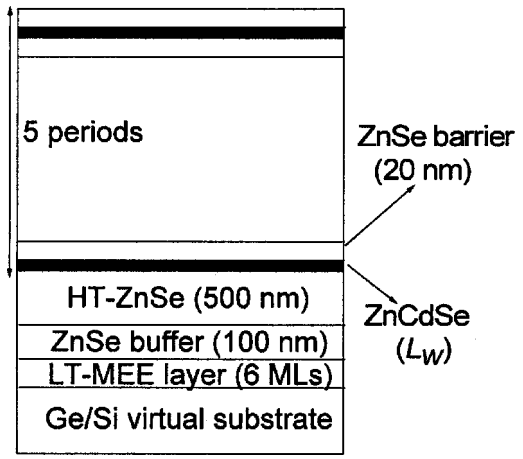


FIG. 1. Schematic illustration of sample structures for ZnCdSe/ZnSe multiple quantum wells.

spectrometer equipped with a thermal electric-cooled photomultiplier tube. Samples were cooled in a closed-cycle refrigerator at 10 K.

## III. RESULTS AND DISCUSSION

Figure 2 shows the normalized LT-PL spectra of samples A, B, C, D, and E, respectively. The PL band near 2.8 eV is attributed to the near-band-edge (NBE) emission, dominated by the emission of neutral donor-bound exciton $D^0X$ (2.791 eV). Other small contributions are due to the emission from the free excitons (2.800 eV) and acceptor-bound excitons (2.787 eV). A narrow line of PL (2.770 eV) is due to the extended structural defects[16] or the recombination

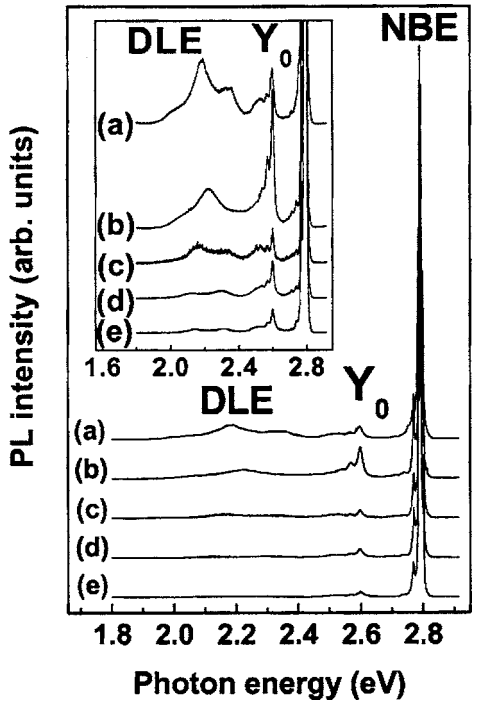


FIG. 2. Photoluminescence spectra of ZnSe epilayers on Ge/Si virtual substrates for different structures: (a) 0°, (b) 4°, (c) 6°, (d) 6°+LT-MEE, (e) and 6°+LT-MEE+buffer. The inset shows the magnified structures of DLE and $Y_0$ bands.

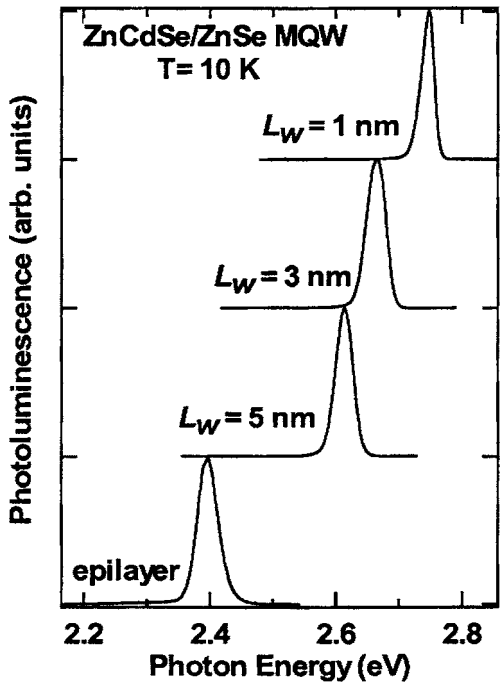


FIG. 3. Low-temperature PL spectra of $Zn_{0.83}Cd_{0.17}Se$ epilayer and $Zn_{0.83}Cd_{0.17}Se$/ZnSe MQWs with various $L_w$'s on a Ge/Si virtual substrate.

from donor states to valence bands.[17] The weak emission band near 2.6 eV, commonly labeled as $Y_0$ line, is related to misfit dislocations.[6] The broad emission band, ranging from 1.9 to 2.5 eV, is associated with DLE, which originated in cation-vacancy related complexes.[18] The inset in Fig. 2 shows the magnified PL spectra, emphasizing the $Y_0$ and DLE structures. The relative intensity ratio of the DLE to excitonic emission in PL spectra has been taken as a parameter of crystal quality.[6] Table I summarized the evaluated ratios of the peak intensity of $D^0X$ to that of the DLE. The peak intensity of the DLE in sample E was successfully reduced by a factor of about 20. As pointed out in Ref. 8, Zn vacancies in a ZnSe epilayer can be reduced using the tilted substrate. The LT-MEE layer and the thermal-annealed LT buffer are expected further to decrease the interdiffusion defects, stacking fault densities, and misfit dislocations, resulting in an improvement of the crystallinity of ZnSe thin films. The intensity of the $Y_0$ line, which correlates to the misfit dislocations, is also weakest in sample E. However, the ZnSe epilayer grown on the 4°-tilted substrate exhibits the strongest $Y_0$ emission and its DLE line shape differs from the others, which fact may attribute to the effect of epilayer tilt.

Table I also shows the full widths at half maximum (FWHMs) of the $D^0X$ emission in samples A–E. It is known that the microscopic fluctuation effects of strain distribution, impurity, and defect density induce potential wells in which excitons can be trapped. Hence, these kinds of inhomogeneities contribute to the broadening in the bound exciton line. Therefore, the narrowest inhomogeneous broadening suggests better crystalline quality in samples on a substrate with a tilted angle of 6°. The PL linewidth of the best-quality sample E can be decreased to 4.9 meV.

The ZnCdSe MQWs grown on a Ge/Si virtual substrate are characterized by PL spectroscopy. Figure 3 shows the

[This article is copyrighted as indicated in the article. Reuse of AIP content is subject to the terms at: http://scitation.aip.org/termsconditions. Downloaded to ] IP: 140.113.38.11 On: Thu, 01 May 2014 02:05:31

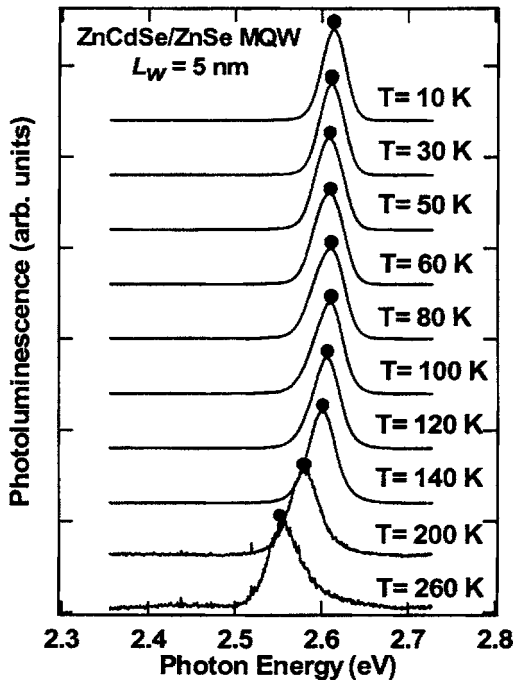


FIG. 4. Temperature-dependent PL spectra of the $Zn_{0.83}Cd_{0.17}Se/ZnSe$ MQW with $L_w$=5 nm. The close circles indicate the peak energy of the emission band.

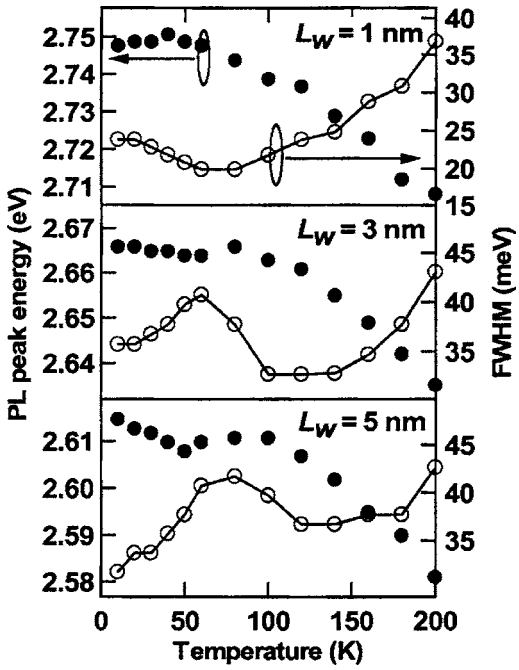


FIG. 5. Evolution of PL peak energy (close circles) and FWHM (open circles) as a function of temperature for the $Zn_{0.83}Cd_{0.17}Se/ZnSe$ MQWs with $L_w$'s of 1, 3, and 5 nm.

LT-PL spectra of $Zn_{1-x}Cd_xSe$ epilayer and $Zn_{1-x}Cd_xSe/ZnSe$ MQWs ($x$=0.17) for various $L_w$'s. An exciton emission band with peak energy of 2.397 eV is observed from the $Zn_{0.83}Cd_{0.17}Se$ epilayer. The PL linewidth of 37 meV is attributed mainly to the alloy composition fluctuation. One-dimensional spatial confinement causes a PL peak blueshift to 2.615 eV for the MQW with a $L_w$ of 5 nm. The emission peak energy of the MQWs is monotonically a decreasing function of $L_w$, which result is consistent with the quantum-size effect. The linewidths of the exciton emission from MQWs with $L_w$'s of 5, 3, and 1 nm are 32, 36, and 26 meV, respectively. This might imply that the inhomogeneous broadening due to chemical disorder and well-depth fluctuation is smallest in the sample of $L_w$=1 nm for this set of MQWs. Further supports of this assignment will be given later.

Temperature-dependence PL measurement was investigated to explore the variation in PL efficiency as the temperature increases. Figure 4 shows typical temperature-dependent PL spectra of the $Zn_{1-x}Cd_xSe/ZnSe$ MQWs ($x$ =0.17) with $L_w$ of 5 nm. The peak energy of excitonic emission exhibits an anomalous dependence on temperature: redshifts in the temperature range from 10 to 50 K, slight blueshifts between 50 and 100 K, and redshifts again beyond 100 K. This temperature-dependent "S-shape" variation of exciton emission has been reported in InGaN (Ref. 19) and ZnO (Ref. 20) QWs. It is caused by the interplay between the relaxation of excitons to the localized states and the inverse delocalization process as the temperature increases. One has to bear in mind that the well material of MQWs studied herein is a ternary alloy. Consequently, the free exciton can be localized by alloy composition disorder and/or well width and well-depth fluctuation at LT.

The PL peak energies as a function of temperature are shown in Fig. 5. The magnitude of the S-shape features, i.e., the redshift and the blueshift energies, varies with $L_w$. This result is probably related to the degree of localization and also to the densities of the localized sites in each MQW. The MQW with the narrowest thickness (1 nm) exhibits fewer localized sites than the other samples. Thus, the redshift-blueshift-redshift change for this MQW becomes less as temperature increases. The dependence of the PL linewidth on temperature was further studied and represented as open circles in Fig. 5, for all of the MQWs. Abnormal evolutions of linewidths were observed at the low temperature. The emission linewidth increased from 10 to 50 K, in which temperature range the emission energy was redshifted, in MQW with $L_w$'s of 3 and 5 nm, as is explained below. The LT emission band, which simultaneously consists of radiative recombination from free and localized excitons, is broadened by the relaxation of localized excitons to available lower-energy localized states as temperature increases, whereas the free excitons are almost unaffected. This broadening increases the PL linewidth and causes a redshift in the peak energy. In the intermediate temperature range from 50 to 100 K, the delocalization effects of trapped excitons overwhelm the reverse relaxation. Therefore, the disappearance of the localized excitonic contribution blueshifts the emission energy and reduces the linewidth. At over 100 K, the mobilized excitons radiatively recombine with respect to the temperature-induced band gap shrinkage and interact with phonons, which broaden the transition level. On the other hand, localized states of the 1 nm MQW is limited, from 10 to 50 K, and delocalization simply reduce the recombination of trapped excitons, narrowing the linewidth of

[This article is copyrighted as indicated in the article. Reuse of AIP content is subject to the terms at: http://scitation.aip.org/termsconditions. Downloaded to ] IP: 140.113.38.11 On: Thu, 01 May 2014 02:05:31

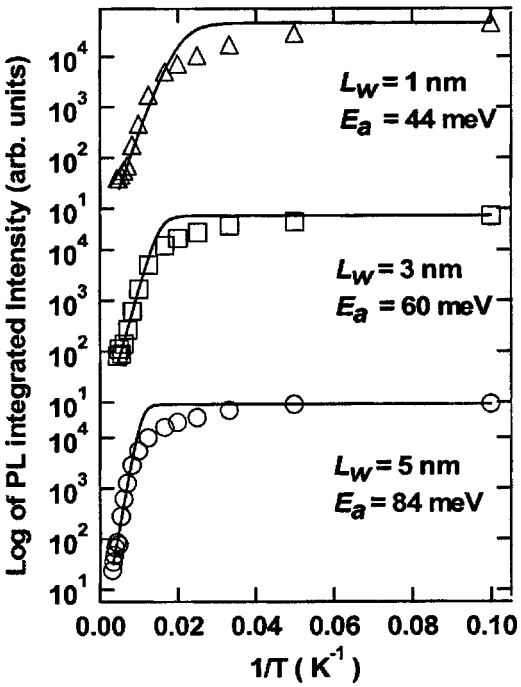


FIG. 6. Arrhenius plots of the integrated PL intensity vs the inverse of temperature for the $ZnSe/Zn_{0.83}Cd_{0.17}Se$ MQWs with $L_w$'s of 1 nm (open triangles), 3 nm (open squares), and 5 nm (open circles). The solid lines represent the fits to Eq. (1). Derived activation energies $E_a$'s were also shown.

the emission band and causing a small blueshift in the peak energy. After 50 K, nearly free excitons dominate the temperature dependence of the PL characteristic.

The thermal activation energy is derived from the Arrhenius plot of the integrated PL intensity of the exciton band against the temperature to investigate the thermal quenching of PL in ZnCdSe MQWs grown on a Ge/Si virtual substrate. The high-temperature range of the PL-integrated intensity variations is given by the general equation[21]

$$I(T) = \frac{I(0)}{1 + A\exp(-E_a/k_BT)}, \tag{1}$$

where $I(T)$ and $I(0)$ are the integrated PL intensities at temperature $T$ and 0 K, respectively. $A$ is a fitting constant that is related to the ratio of the radiative lifetime to the nonradiative lifetime[21] and $k_B$ is the Boltzmann constant. Notably, the radiative rate is assumed to be constant within temperature in this model. One activation energy $E_a$ was derived for the temperature range above 120 K. The fitting curves and the values of $E_a$ obtained are shown in Fig. 6. The temperature dependence of emission intensity in the fitting at LT is ignored because the emission band is composed of contributions from both localized and free excitons.

In general, the quenching of PL intensity with temperature can be explained by the thermal emission of the carriers out of a confining potential with an activation energy correlated with the depth of the confining potential. The temperature-induced quenching of PL intensity in MQW structures at high temperature is primarily due to the thermal emission of charge carriers out the confined QW states into barrier states.[22] The difference between the band gaps of the well and the barrier of this MQW structures is approximately 250 meV.[23] The confined energies of the conduction and the valence bands are estimated to be in the ranges of 213–163 and 37–87 meV, considering a band-offset ratio of 0.65–0.85.[24] At a high temperature, $E_a$ increases from 44 to 84 meV as $L_w$ increases. The enhancement of $E_a$ for a large $L_w$ is presumably due to the decrease of quantized subband energy. This leads to a large energy difference between QW states and barrier states, consequently enlarging the $E_a$ for thermal emission out of carriers from QW states.

## IV. CONCLUSIONS

The deep level emission of ZnSe epilayers grown on the tilted-$Ge/Ge_{0.95}Si_{0.05}/Ge_{0.9}Si_{0.1}/Si$ virtual substrate was investigated. The PL spectrum of ZnSe epilayers grown on a 6°-tilted Ge/Si virtual substrate with an inserted LT-MEE layer and an *in situ* annealed LT-ZnSe buffer layer exhibits the maximum intensity ratio of bound exciton emission to the deep level emission. Quantum-confinement effect of ZnCdSe MQWs grown on a Ge/Si virtual substrate was identified in the PL spectroscopy. The evolution of exciton emission peak energy and FWHM as a function of temperature suggests lower density of localized states in sample with $L_w$ of 1 nm. Thermal quenching of excitonic emission intensity for ZnCdSe MQWs grown on Ge/Si structures was governed by the thermal activation of carriers from QW confined states into barrier states.

## ACKNOWLEDGMENT

This work was supported by the National Science Council of Taiwan under the grant numbers of NSC-93-2112-M-009-031 and NSC94-2112-M-009-013.

[1] M. A. Haase, J. Qiu, J. M. Depuydt, and H. Chang, Appl. Phys. Lett. **59**, 1272 (1991).
[2] D. Eason *et al.*, J. Cryst. Growth **150**, 718 (1995).
[3] R. D. Bringans, D. K. Biegelsen, L. E. Swartz, F. A. Ponce, and J. C. Tramontana, Phys. Rev. B **45**, 13400 (1992).
[4] M. K. Lee, M. Y. Yeh, and C. C. Chang, Appl. Phys. Lett. **55**, 1850 (1989).
[5] M. Yokoyama, N. T. Chen, and H. Y. Ueng, J. Cryst. Growth **212**, 97 (2000).
[6] M. López-López, V. H. Méndez-García, M. Meléndez-Lira, J. Luyo-Alvarado, M. Tamura, K. Momose, and H. Yonezu, Phys. Status Solidi B **220**, 99 (2000).
[7] G. L. Luo, T. H. Yang, E. Y. Chang, C. Y. Chang, and K. A. Chao, Jpn. J. Appl. Phys., Part 2 **42**, L517 (2003).
[8] T. H. Yang, C. S. Yang, G. Luo, W. C. Chou, T. Y. Yang, E. Y. Chang, and C. Y. Chang, Jpn. J. Appl. Phys., Part 2 **43**, L811 (2004).
[9] J. M. Gaines, J. Petruzzello, and B. Greenberg, J. Appl. Phys. **73**, 2835 (1992).
[10] J. S. Song, J. H. Chang, S. K. Hong, M. W. Cho, H. Makino, T. Hanada, and T. Yao, J. Cryst. Growth **242**, 95 (2002).
[11] M. C. Kuo *et al.*, Jpn. J. Appl. Phys., Part 2 **43**, 5145 (2004).
[12] U. Lunz, J. Kuhn, F. Goschenhofer, U. Schüssler, S. Eiufeldt, C. R. Becker, and G. Landwehr, J. Appl. Phys. **80**, 6861 (1996).
[13] R. Cingolani *et al.*, Phys. Rev. B **51**, 5176 (1995).
[14] H. J. Lozykowski and V. K. Shastri, J. Appl. Phys. **69**, 3235 (1991).
[15] M. Godlewski, J. P. Bergman, B. Monemar, E. Kurtz, and D. Hommel, Appl. Phys. Lett. **69**, 2843 (1996).

[This article is copyrighted as indicated in the article. Reuse of AIP content is subject to the terms at: http://scitation.aip.org/termsconditions. Downloaded to ] IP: 140.113.38.11 On: Thu, 01 May 2014 02:05:31

[16]K. Shahzad, J. Petruzzello, D. J. Olega, and D. A. Cammack, Appl. Phys. Lett. **57**, 2452 (1990).
[17]C. S. Yang, D. Y. Hong, C. Y. Lin, W. C. Chou, C. S. Ro, W. Y. Uen, W. H. Lan, and S. L. Tu, J. Appl. Phys. **83**, 2555 (1998).
[18]X. B. Zhang, K. L. Ha, and S. K. Hark, J. Cryst. Growth **223**, 528 (2001).
[19]Y. H. Cho, G. H. Gainer, A. J. Fischer, J. J. Song, S. Kreller, U. K. Mishra, and S. P. DenBaars, Appl. Phys. Lett. **73**, 1370 (1998).
[20]T. Makino *et al.*, Appl. Phys. Lett. **78**, 1979 (2001).
[21]M. Leroux, N. Grandjean, M. Laugt, J. Massies, B. Gil, P. Lefebvre, and P. Bigenward, J. Appl. Phys. **86**, 3721 (1999).
[22]E. Tournié, C. Morhain, M. Leroux, C. Ongaretto, and J. P. Fourie, Appl. Phys. Lett. **67**, 103 (1995).
[23]The band gap energy of ZnSe at a low-temperature limit (0*T*) is 2.82 eV. Calculate the band gap of $Zn_xCd_{1-x}Se$ ($x$=0.17) using the method described in Ref. 12; we get a band offset of 250 meV for 0*T*.
[24]R. L. Gunshor and A. V. Nurmikko, *II–VI Blue Green Light Emitters: Device Physics and Epitaxial Growth* (Academic, Boston, 1997), p. 179.

[This article is copyrighted as indicated in the article. Reuse of AIP content is subject to the terms at: http://scitation.aip.org/termsconditions. Downloaded to ] IP: 140.113.38.11 On: Thu, 01 May 2014 02:05:31